

Imaging hyporheic zone solute transport using electrical resistivity

Adam S. Ward,^{1*}
Michael N. Gooseff¹ and
Kamini Singha²

¹ Department of Civil and Environmental Engineering, The Pennsylvania State University, University Park, PA 16802, USA
² Department of Geosciences, The Pennsylvania State University, University Park, PA 16802, USA

*Correspondence to:

Adam S. Ward, Department of Civil and Environmental Engineering, The Pennsylvania State University, 212 Sackett Building, University Park, PA 16802, USA.

E-mail: asward@psu.edu

Additional Supporting Information may be found in the online version of this article.

Abstract

Traditional characterization of hyporheic processes relies upon modelling observed in-stream and subsurface breakthrough curves to estimate hyporheic zone size and infer exchange rates. Solute data integrate upstream behaviour and lack spatial coverage, limiting our ability to accurately quantify spatially heterogeneous exchange dynamics. Here, we demonstrate the application of near-surface electrical resistivity imaging (ERI) methods, coupled with experiments using an electrically conductive stream tracer (dissolved NaCl), to provide *in situ* imaging of spatial and temporal dynamics of hyporheic exchange. Tracer-labelled water in the stream enters the hyporheic zone, reducing electrical resistivity in the subsurface (to which subsurface ERI is sensitive). Comparison of background measurements with those recording tracer presence provides distributed characterization of hyporheic area (in this application, $\sim 0.5 \text{ m}^2$). Results demonstrate the first application of ERI for two-dimensional imaging of stream-aquifer exchange and hyporheic extent. Future application of this technique will greatly enhance our ability to quantify processes controlling solute transport and fate in hyporheic zones, and provide data necessary to inform more complete numerical models. Copyright © 2010 John Wiley & Sons, Ltd.

Key Words hyporheic; geophysics; non-Fickian; solute transport; tomography; stream tracer

Introduction

The exchange of stream water with near-stream aquifers and the associated physical, chemical and biological processes have been shown to provide a number of ecosystem services (Brunke and Gonser, 1997). The quantification of these hyporheic processes, however, has been limited by our ability to understand the magnitude, extent and spatial variability of exchange between the stream channel and the hyporheic zone. Improved characterization of these exchange processes in space and time is, therefore, critical to our understanding of the role of the hyporheic zone in stream ecosystem and water quality function.

Stream tracer studies are frequently used to estimate the interaction of the mobile stream domain with the less mobile hyporheic zone (Stream Solute Workshop, 1990). Such studies produce in-stream breakthrough curves that are a product of integrated transport processes over a reach (e.g. advection and dispersion), and exhibit tailing behaviour commonly attributed to solute exchange between the stream and near-stream aquifers or in-stream zones of low velocity (Wagner *et al.*, 1996). Stream solute transport modelling often yields estimates of the reach-representative extent of lumped mobile and immobile zones and exchange rates (e.g. Wagner and Harvey, 1997), which rely on observations in the surface mobile domain to characterize less mobile domains. Such results have been identified as not physically meaningful (Marion *et al.*, 2003; Wondzell, 2006). Further limiting our understanding of the hyporheic zone from these models are the problems of tracer experiment sensitivity to more than storage zone processes (Harvey *et al.*, 1996), and the difficulty in accurately estimating precise storage zone characteristics. These discrepancies are due in part to the representation of transient storage as a single, well-mixed zone and are sensitive to monitoring location with respect

Received 25 August 2009
Accepted 23 February 2010

to the flowpaths. Installation of extensive and invasive monitoring well networks provides point-verification of exchange, but ultimately lack spatial resolution and representation of extensive spatial coverage of the solute transport processes. Data from monitoring wells rarely agree with predictions based on in-stream solute transport modelling (Harvey *et al.*, 1996; Wondzell, 2006).

Understanding solute transport in the subsurface ultimately requires quantification beyond classical advection and dispersion processes. Observations of tailing behaviour that cannot be described by these processes alone have led to the conceptualization of mass transfer among a spectrum of domains ranging from very mobile (i.e. stream) to immobile (i.e. dead-end pore space) (Goltz and Roberts, 1986). The subsurface domain itself, often viewed by stream solute models as a lumped domain that is completely immobile, is instead conceptualized as including a mobile domain (e.g. connected pore space modelled with advection and dispersion) and immobile domain (e.g. fluid in poorly connected pore space). Local rate-limited mass transfer among domains is conceived as controlling the tailing behaviour observed for both the subsurface mobile domain and stream solute transport. Direct sampling in monitoring wells provides only an assessment of mobile water in the subsurface. Complete quantification of solute transport must, then, attempt to quantify solute presence in subsurface immobile domains as well as those domains more traditionally sampled (i.e. the total distribution of tracer in the subsurface).

To overcome the limitations inherent in stream solute transport modelling and current hyporheic zone assessment methods, we propose the use of electrical resistivity imaging (ERI) to estimate the spatial distribution of introduced ionic tracers in the hyporheic zone. ERI is a direct-current (or low-frequency alternating-current) method that can be used to estimate the spatial and temporal distribution of subsurface electrical resistivity (the reciprocal of electrical conductivity). The introduction of an electrically conductive fluid decreases the bulk electrical resistivity of the soil–water matrix. ERI has been used to successfully image the exchange of seawater with a freshwater sand aquifer in a tide-water stream (Acworth and Dasey, 2003) and groundwater discharge into streams (Nyquist *et al.*, 2008). Crook *et al.* (2008) used cross-borehole ERI and in-stream longitudinal profiles to assess the subsurface sediment deposits in two streams, informing predictions of hyporheic exchange with estimates of subsurface architecture in streams, primarily focused on the size and distribution of alluvial deposits. ERI allows for the assessment of total concentration distribution within the mobile and immobile zones (Day-Lewis and Singha, 2008). Singha *et al.* (2007) demonstrated the use of ERI to directly quantify mass transfer in heterogeneous aquifers during a push–pull tracer test in fractured porous media. More recently, Singha *et al.* (2008) demonstrated numerically that ERI could be coupled with an analysis of temporal moments to quantify solute exchange between the stream and less mobile domains. None of these studies, however, leverage ERI to assess surface–subsurface

exchange dynamics. This is the first study, to the best of our knowledge, quantifying temporal dynamics of surface–subsurface exchange and providing a framework for quantifying hyporheic extent at the field scale.

Here, we apply direct-current geoelectrical techniques to quantify the extent of exchanging tracer from the surface into the subsurface. Because ERI is sensitive to both mobile and immobile zone concentrations, the method more completely represents surface–subsurface exchange mechanisms than point measurements in monitoring wells. Exchange of the tracer-labelled stream water with subsurface fluids reduces the electrical resistivity of the area actively communicating with the stream. Our research objectives are (1) to demonstrate the ability of ERI to quantify hyporheic extent and (2) to compare in-stream concentration with hyporheic extent. Inverted resistivity tomograms will be used to image, for the first time in a field setting, the extent of hyporheic exchange in the subsurface. Spatially distributed assessment of solute transport in the subsurface provides insight to subsurface heterogeneity and localized processes that would otherwise be averaged over the reach using traditional characterization methods.

Methods

Site description

We conducted a stream tracer experiment in stream #1 of the Leading Ridge Watershed Research Unit in central Pennsylvania, USA. The watershed ranges in elevation from 270 to 440 m above the mean sea level. Leading Ridge stream #1 is a cobble-bedded stream with a gradient of 5% through the study reach, draining a catchment of approximately 0.43 km². The stream reach is 1.5–2.0 m wide and 0.1–0.2 m deep, on average.

Tracer injection

We conducted a constant rate injection (~1 ml/s) of dissolved NaCl (61.9 mS/cm) for 20.8 h (starting 17:04 on 31 October 2008) immediately downstream of a weir at the head of the study reach (0 m). Tracer was injected from a single, well-mixed reservoir prepared prior to the injection. Injection rate was constant, with volumetric flow rate of the injection verified before and after the injection period. In-stream conductivity measurements were collected upstream of the injection point, and at the geophysical transect (located ~70 m downstream of the weir, Figure 1). The tracer breakthrough curve presented here is from a replicate experiment completed in mid-November, because of a failure of in-stream data loggers during the October 2008 experiment; however, conditions for the two injections were similar, with an average flow of 0.6 l/s at the upstream weir for both injections. The plateau for the in-stream breakthrough curve presented was extended by 1.3 h to account for the difference in injection duration between the October and November trials. The in-stream breakthrough curve is presented only as representative of arrival and departure times for the

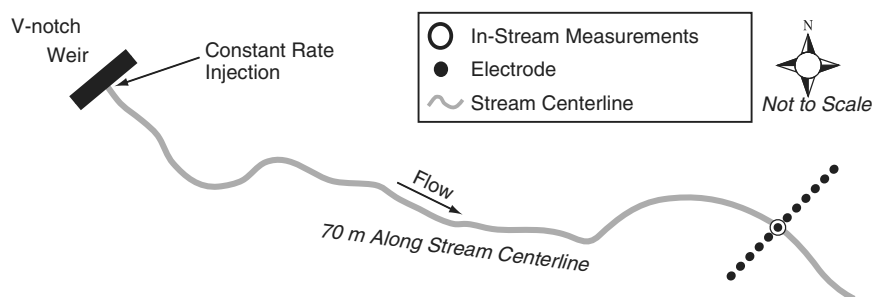


Figure 1. A constant rate tracer injection was performed at the Leading Ridge Experimental Watershed near State College, PA, USA. The injection of NaCl to the surface water occurred immediately downstream of a V-notch weir, used to measure discharge. Geophysical data were collected approximately 70 m downstream of the injection, using 12 electrodes set transverse to the stream at 2 m typical spacing. In-stream tracer concentration data were collected at the geophysical transect

tracer in the stream, as the focus of this study is the interpretation of electrical resistivity data.

Electrical resistivity imaging

ERI data were collected with an IRIS Syscal Pro Resistivity Meter, using a dipole–dipole geometry with 166 quadripoles collected across 12 electrodes set at 2 m spacing (Figure 1) to balance the depth of penetration and good spatial resolution with high temporal sampling. Background data collection consisted of collecting four sets of pre-injection measurements along the transect. Data collection continued for 22.8 h after the injection ended to monitor the substrate flushing of the conservative tracer. During collection, replicate measurements were collected and stacked (averaged) twice by the instrument for data within 3% difference of one another. If this quality threshold was not met, a third measurement was included in the average. The average standard deviation between replicate measurements was 0.085 Ωm (0.08%) for the 35 856 individual measurements collected for the transect. Data were collected at approximately 1.5-h intervals to avoid temporal smearing.

Inversion of ERI data

Inverted models of electrical resistivity are smooth representations of the subsurface due to the physics of diffusion and the data inversion process (Day-Lewis *et al.*, 2005). Although these inversions cannot represent the small-scale heterogeneity of the subsurface given the regularization in inversion, they can be used to approximate relative changes in the area of the subsurface where the tracer is present. Because results are sensitive to a particular inversion scheme, model settings and inherent assumptions in the model code (seeking the smoothest model that the data will accommodate, for example), the same inversion settings were used for each time step. Inverted resistivities were exported from EarthImager2D (Advanced Geosciences, Inc.) using inversion block sizes ranging from 0.5 to 1.0 m horizontal and 0.07 to 0.18 m vertical. To parse meaningful changes in bulk resistivity from error in the data collection and modelling scheme, we chose a threshold of 3.5% decrease in bulk resistivity. This value is greater than the error in the data collected, and attempts to account for model and structural error,

which can be difficult to quantify. Interpretation of results is sensitive to the threshold chosen (see Section on Discussion and Figure 3A).

ERI inversion was completed for each transect using EarthImager2D. Background (pre-injection) data were used as a baseline for comparison of data collected during the injection. Using EarthImager2D's time-lapse inversion, differences between baseline resistance and subsequent (during injection) data sets were inverted using the background data as a priori information (the starting model for each time step), allowing faster convergence and sensitivity to smaller changes in bulk resistivity. Inversion results produced a root mean square error of less than 2% (mean 1.47%) for all time steps.

Results

Results of the ERI models (as percentage difference from the background resistivity) are presented for selected time steps (Figure 2, cross-sections transverse to the stream with flow directed out of the page). The differenced models were processed to calculate an approximate hyporheic area communicating with the stream, based on bulk resistivity decreases due to tracer presence. Time-lapse imaging of solute tracer (Figure 2) shows the presence of tracer both below the stream ($X = 10\text{--}12\text{ m}$) and on the inside of the meander bend ($X = 4\text{ m}$). Images of time-lapse visualization of electrical resistivity are available online (Supporting Information). Hyporheic cross-sectional area ranges from 0.0 to approximately 0.5 m^2 during the injection for a threshold of 3.5%. We note that the estimated hyporheic area is dependent on this choice of threshold. Because the 'true' threshold value is difficult to quantify and likely spatially and temporally variable, we consider a simple sensitivity analysis, which shows while the magnitude changes, the same areal trends are present across a range of threshold values (Figure 3A). Bimodal response of the subsurface through time for lower threshold values (2% and 3.5%, Figure 3A) suggests observed in-stream concentration histories alone cannot predict the subsurface solute transport. Average horizontal distribution (Figure 3B) is based on the ERI inversion grid and shows a secondary emergence of the tracer at $X = 4\text{ m}$ (Figure 2F), which we interpret as an abandoned streambed from a past

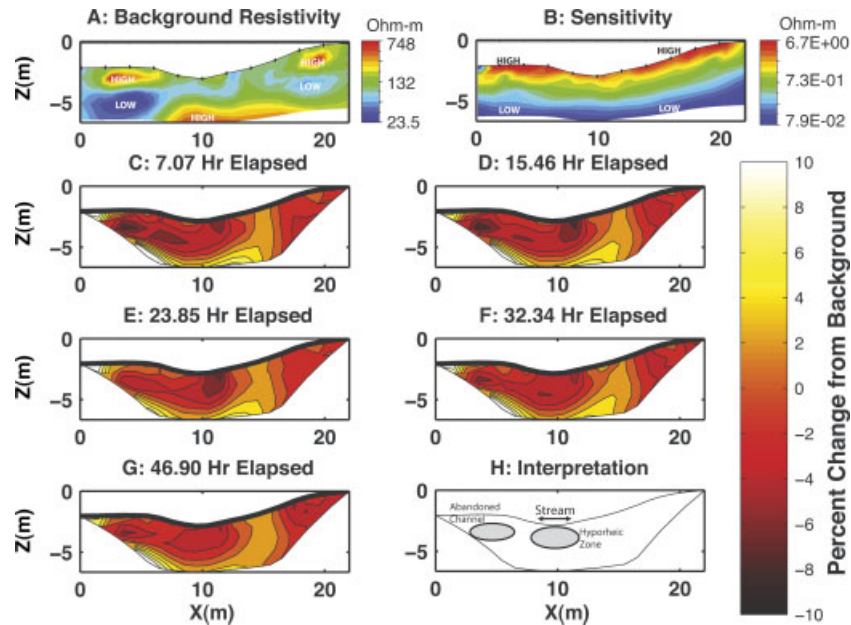


Figure 2. (A) Pre-injection electrical resistivity model. Transects shown are perpendicular to the stream, with flow directed out of the page. We propose that areas of high resistivity at $X = 2\text{--}4$ m at an elevation of -3 m local datum are representative of a cobble-bed that was abandoned during lateral migration of the stream (currently located inside a meander bed). Bedrock is observed in the model at $X = 7\text{--}18$ m and elevations below -5 m local datum. Low resistivity areas ($2 < X < 6$, $4 < Z < 7$) are likely a product of low model sensitivity (Panel B) in this same region. (B) Model sensitivity as a function of physical location, from EarthImager2D. Note the areas of highest sensitivity near the surface, and decreasing sensitivity with depth. (C–G) Time-lapse ERI results, at time elapsed after beginning the conservative solute injection. Resolution of the geophysical image decreases at the edges. Grid cell colour indicates the percentage change in bulk resistivity from background conditions. (C and D) Decrease in bulk resistivity in the subsurface due to tracer presence. (E) Tracer is flushed from the subsurface. (F) Second increase in flowpath centred at $X = 4$ m (see 2% threshold curve in panel A). (G) Flushing of tracer from the subsurface. (H) Interpretation of resistivity images. We hypothesize the decrease centred at $X = 4$ m is due to an abandoned stream channel, given its elevation equal to that of the stream and location on the inside of a meander bed

alignment, where the cobble-bed transports solute more rapidly than the surrounding substrate. We interpret the second mode (Figure 3A) as a result of a second ‘pulse’ of tracer past the geophysical transect, moving through slower flowpaths. It is reasonable to hypothesize that the stream migrated laterally in the valley, but maintained its elevation. Average vertical distribution of the tracer (Figure 3C) shows the solute below the streambed and saturated bank areas near the stream.

Discussion

We develop a 2D technique to detect the presence of the salt tracer in the subsurface, simultaneously assessing both mobile and immobile domains, which has been previously impossible using in-stream, monitoring well, or modelling techniques. Our results demonstrate a peak hyporheic zone of approximately 0.5 m^2 for the 20.8 h injection for an assumed 3.5% threshold in the change in resistivity. Based on the quality of our data and ability to match those in inversion, we believe that a threshold change of 3.5% is adequate to distinguish meaningful changes in bulk resistivity from those due to data noise and model error, though results are sensitive to the threshold chosen (Figure 3A). We acknowledge that calculations of the hyporheic zone area from ERI data are sensitive to the error in the data collection and the resolution of the ERI method. Despite these uncertainties, which are inherent in all geophysical inversions, these data enhance understanding of localized exchange processes. ERI data

provide more complete subsurface solute transport data than could be collected with standard measurements.

For future studies, analysis of the threshold chosen should be completed and the threshold compared with the known error in both data collection and inversion; we selected 3.5% based on these factors, and explored the sensitivity of results to the chosen threshold for interpretation. It is important to note that the overall trends in hyporheic area remain constant between chosen thresholds. Application of ERI to hyporheic studies holds the potential to more accurately quantify interactions between streams and hyporheic zones. ERI methods provided a distributed assessment of solute transport in the hyporheic zone, a data set that is impossible to collect using traditional and invasive point measurements. We expect that ERI results can be used to characterize transport behaviour by illuminating the temporal dynamics of flowpaths and their deviation from mobile in-stream and subsurface observations. In-stream and subsurface tracer concentration are correlated during the injection plateau, but subsurface dynamics produce a different tailing, and a secondary mode for some sensitivity thresholds at later times. Thus, while the in-stream tracer data appear to be insensitive to small fluxes of tracer coming back to the stream (Harvey *et al.*, 1996; Wondzell, 2006), the ERI data provide continued measurement of tracer in the hyporheic zone. Geophysical data collected during this tracer study guided the installation of monitoring wells for subsequent tracer studies (Ward, unpublished data),

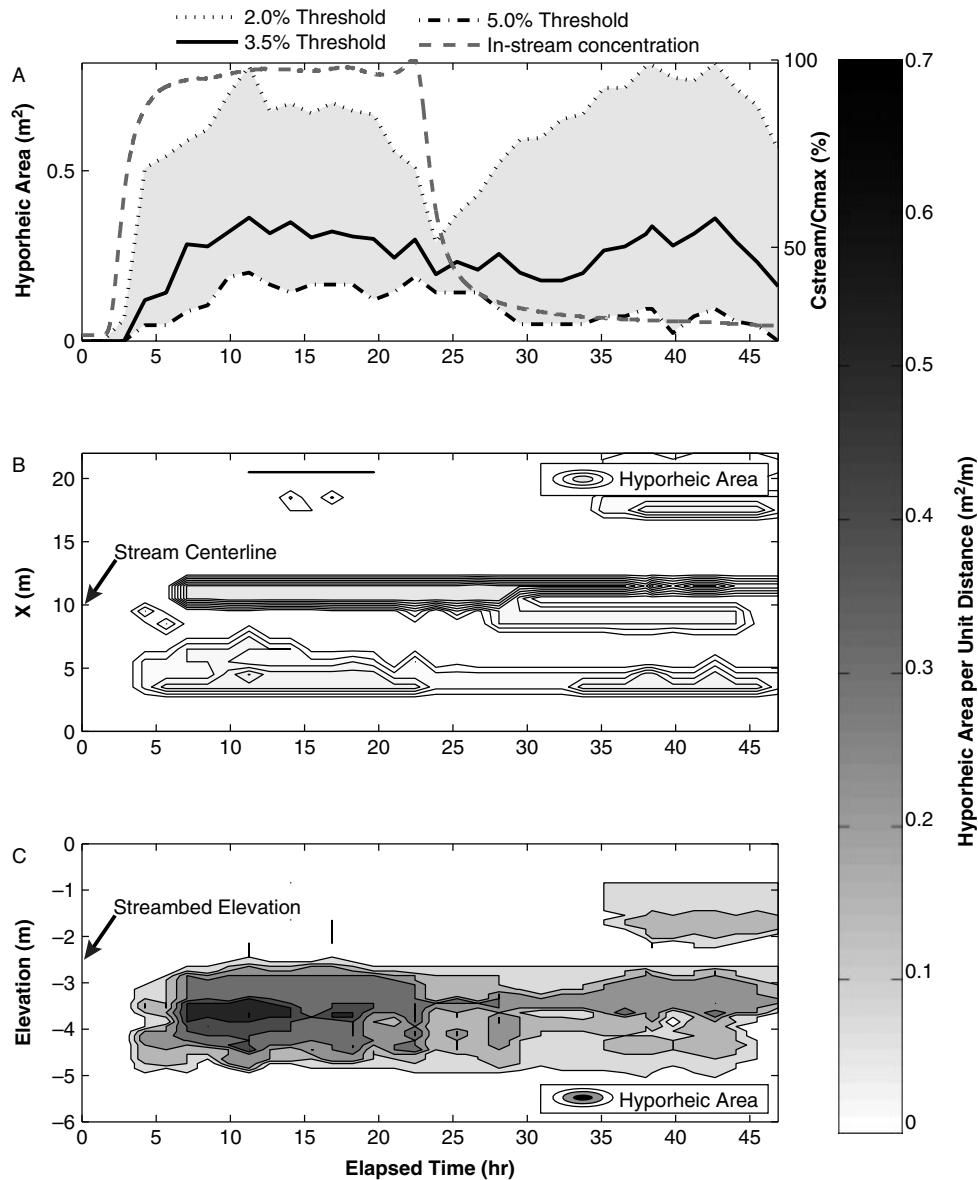


Figure 3. (A) Storage zone area versus time for the transect, using a threshold of minimum 3.5% decrease in resistivity. Two to five percentage threshold range is indicated by the shading. In-stream concentration (dashed grey) is normalized to maximum concentration, and representative of in-stream processes during the geophysical data collection. Note the second mode of tracer concentration, correlating with a flowpath centred at $X = 4$ m. (B) Contour plot of the horizontal distribution of resistivity decreases (and thus tracer presence) in the subsurface through time. $X = 0$ m corresponds to the left-most and $X = 22$ m the right-most data presented in Figure 2. The changes from $X = 15$ m to $X = 22$ m are attributed to noise in the data set, as these locations are substantially above the channel elevation and in a poorly resolved area of the transect. (C) Contour plot of the vertical distribution of resistivity decreases (and thus tracer presence) in the subsurface through time. Note the changes remain within 1 m of streambed elevation, at the expected vertical location hyporheic zone

which confirmed the presence of the tracer in monitoring wells at approximately 25, 50 and 65–75 cm below the streambed. Confirmation of tracer presence during subsequent studies suggests ERI accurately identified the tracer location in the subsurface.

Pre-injection resistivity models (Figure 2A) consistently identify areas of high resistivity at an elevation of about -6 m (local datum) representing the shallow bedrock below the valley soils, consistent with the observations of 0.5–2.0 m soil depth in the watershed (Lynch and Corbett, 1989). The area of high resistivity located at $X = 3$ – 5 m at an elevation of -3 m (local datum) is at the same horizontal and vertical location as the observed

preferential flowpath during the solute injection, supporting our interpretation that the preferential flowpath is an abandoned cobble streambed.

Collection and processing of data during this experiment yielded meaningful results and provides a foundation upon which the technique may be refined and improved. Because electrical current travels in three dimensions, the problem of dimensionality must be considered for a two-dimensional array. Collecting data across and between multiple transects would allow the construction of a fully three-dimensional image of hyporheic zones and would eliminate dimensionality concerns. Future research will correlate subsurface mobile domain concentration with changes in bulk resistivity,

which would lend itself to additional interpretation of ERI data and model results. Traditional modelling of solute transport with transient storage assumes a constant value to represent the size of a lumped immobile domain (i.e. lumped transient storage) with a concentration that changes through time. Here, we demonstrate that not only does the spatial distribution of tracer concentration change in the hyporheic zone through time but also the physical size of the hyporheic zone is temporally variable. Furthermore, this method has the potential to inform new models of mobile–immobile solute transport (e.g. Zhang *et al.*, 2006) that account for the spatial and temporal distributions of both mobile and immobile solutes. This spatial resolution provides a distinct advantage in predicting the fate of water quality constituents over those that fit only mobile solute data.

Conclusions

We used ERI to characterize the physical extent of the hyporheic zone during a conservative tracer injection to provide a fully distributed characterization of hyporheic solute concentration in both the mobile and immobile domains in the subsurface. For the first time, direct and fully distributed assessment of the arrival of tracer into the hyporheic zone, and assessment of subsurface areal trends, is possible. The data collection schemes used here were chosen for efficiency; the ability to collect additional data with better spatial or temporal resolution will lead to improved quantification of the dynamics of the hyporheic zone. This work demonstrates the first field-application of ERI to actively image stream tracers as a viable technology for the assessment of to quantify hyporheic extent and exchange dynamics.

The field and modelling techniques of this study provide spatially distributed assessment of solute transport in the hyporheic zone, including the ability to assess mobile and immobile domains. Through time-lapse ERI inversion, we are able to understand both spatial and temporal exchange characteristics and interpret the physical extent of the hyporheic zone. Results demonstrate spatial variability and temporal trends that have been otherwise unobserved in hyporheic studies. Our understanding of the complex biogeochemical processes in the hyporheic zone must be founded upon an understanding of hyporheic exchange processes, which we are only beginning to elucidate more accurately with this technique.

This work demonstrates the potential of ERI for studies of hyporheic exchange in small streams. We identified limitations in the interpretation of ERI for quantifying hyporheic extent, and demonstrated the need for at least a basic level of sensitivity analysis. The apparent increase in solute concentration at some locations ($X = 4$ m in Figure 2F), despite the decreasing in-stream concentration at this time, (Figure 3A) demonstrates the inability of in-stream concentration histories alone to predict solute presence in the subsurface due to dramatically different transport time scales.

Acknowledgements

The authors acknowledge the dedication of Julianne Hagarty and Nathan Barber in field data collection and geophysical data processing. Our thanks to Dr Elizabeth Boyer and her support of this work at the Leading Ridge Experimental Watershed site. NSF Grants EAR - 0747629 and EAR - 0911435 supported this work.

References

- Acworth R, Dasey G. 2003. Mapping of the hyporheic zone around a tidal creek using a combination of borehole logging, borehole electrical tomography and cross-creek electrical imaging, New South Wales, Australia. *Hydrogeology Journal* **11**: 368–377.
- Advanced Geosciences I. 2008. Instruction Manual for EarthImager 2D v2.3-0.
- Brunke M, Gonser T. 1997. The ecological significance of exchange processes between rivers and groundwater. *Freshwater Biology* **37**: 1–33.
- Crook N, Binley A, Knight R, Robinson D, Zarnetske J, Haggerty R. 2008. Electrical resistivity imaging of the architecture of sub-stream sediments. *Water Resources Research* **44**: W00D13.
- Day-Lewis F, Singha K. 2008. Geoelectrical inference of mass transfer parameters using temporal moments. *Water Resources Research* **44**: W05201.
- Day-Lewis F, Singha K, Binley A. 2005. Applying petrophysical models to radar travel time and electrical resistivity tomograms: resolution-dependent limitations. *Journal of Geophysical Research* **110**: B08206.
- Goltz M, Roberts P. 1986. Three-dimensional solutions for solute transport in an infinite medium with mobile and immobile zones. *Water Resources Research* **22**: 1139–1148.
- Harvey JW, Wagner BJ, Bencala KE. 1996. Evaluating the reliability of the stream tracer approach to characterize stream–subsurface water exchange. *Water Resources Research* **32**: 2441–2451.
- Lynch J, Corbett E. 1989. Hydrologic control of sulfate mobility in a forested watershed. *Water Resources Research* **25**: 1695–1703.
- Marion A, Zaramella M, Packman A. 2003. Parameter estimation of the transient storage model for stream–subsurface exchange. *Journal of Environmental Engineering* **129**: 456–463.
- Nyquist J, Freyer P, Toran L. 2008. Stream bottom resistivity tomography to map ground water discharge. *Ground Water* **46**: 561–569.
- Singha K, Day-Lewis F, Lane J. 2007. Geoelectrical evidence of bicontinuum transport in groundwater. *Geophysical Research Letters* **34**: L12401.
- Singha K, Pidlisecky A, Day-Lewis F, Gooseff M. 2008. Electrical characterization of non-Fickian transport in groundwater and hyporheic systems. *Water Resources Research* **44**: W00D07.
- Stream Solute Workshop. 1990. Concepts and Methods for Assessing Solute Dynamics in Stream Ecosystems. *Journal of the North American Benthological Society* **9**: 95–119.
- Wagner BJ, Bencala KE, Harvey JW. 1996. Evaluating the reliability of the stream tracer approach to characterize stream–subsurface water exchange. *Water Resources Research* **32**: 2441–2451.
- Wagner BJ, Harvey JW. 1997. Experimental design for estimating parameters of rate-limited mass transfer: analysis of stream tracer studies. *Water Resources Research* **33**: 1731–1741.
- Wondzell SM. 2006. Effect of morphology and discharge on hyporheic exchange flows in two small streams in the Cascade Mountains of Oregon, USA. *Hydrological Processes* **20**: 267–287.
- Zhang Y, Baeumer B, Benson D. 2006. Relationship between flux and resident concentrations for anomalous dispersion. *Geophysical Research Letters* **33**: L18407.